Donor-Acceptor Spiro-Compounds – Syntheses, Structures, and Electronic Properties☆

Rolf Gleiter*, Herbert Hoffmann, Hermann Irngartinger, and Matthias Nixdorf

Organisch-Chemisches Institut der Universität Heidelberg,
Im Neuenheimer Feld 270, D-69120 Heidelberg, Germany

Received April 27, 1994

Key Words: Spiro interaction / Donor-acceptor molecules / PE spectroscopy / UV/Vis spectroscopy

The six donor-acceptor spiro compounds spiro[1,3-dioxolane-2,2'-indan]-1',3'-dione (**8**), spiro[indan-2,2'-[1,3]oxathiolane]-1,3-dione (**9**), spiro[1,3-dithiolane-2,2'-indan]-1',3'-dione (**10**), spiro[1,3-benzodioxole-2,2'-indan]-1',3'-dione (**11**), 5-methylspiro[1,3-benzodithiole-2,2'-indan]-1',3'-dione (**12**), and spiro[indan-2,2'-naphtho[2,3-*d*]-1,3-dioxole]-1,3-dione (**13**) have been prepared. Their He(I) photoelectron spectra and their UV/Vis spectra have been investigated. A comparison between the first PE bands of the spiro compounds and the corresponding fragments indicates only a very weak interaction between both parts. The UV/Vis spectra of **11**–**13** show a moderate long-wavelength shift of the first band as compared to 1,3-indandione. This band is assigned to a transition from the HOMO(π), localized at the donor fragment, to the LUMO(π^*) of the acceptor moiety (charge transfer). X-ray investigations of **8**–**10** and **13** show no interaction between the two perpendicularly arranged moieties.

The connection of two perpendicularly oriented π systems by a tetrahedral center leads to a particular type of homoconjugation which has been termed spiro conjugation[1–3]. Spiro conjugation has been studied mainly in highly symmetrical (D_{2d}) cases such as spiro[4.4]nonatetraene (**1**)[4] and related species[5] as well as heterocyclic systems (**2** and **3**)[3,5,6]. The investigations of less symmetrical systems like the spiro[4.2]heptatriene derivative **4**[7] and several heterocyclic derivatives **5**–**7**[1,8–10] have revealed less clear-cut evidence for spiro conjugation, although the long-wavelength shifts in their electronic spectra have been ascribed to this effect. In continuation of our long-standing interest in the electronic structure of spiro systems[3,6,7,11] we report in this paper on spiro compounds with a donor and acceptor fragment. The compounds investigated are **8**–**13**.

Together with these systems we discuss the spectroscopic properties of various fragments such as **14**–**20**.

Synthesis

The synthesis of **8** has been reported[1,8]. The synthesis of **9**–**13** follows straightforward procedures involving reaction of 2,2-dichloroindan-1,3-dione (**21**)[12] with the corresponding alcohols or thiols (**22**, **23**). For the synthesis of **9** and **10** this is shown in Scheme 1. Similarly, **11**–**13** have been prepared from **21** and the corresponding dihydroxy compounds and dithiols, respectively.

Structural Investigations

The structures of compounds **8**–**10** and **13** are investigated by X-ray analysis. The resulting geometrical parameters are given in Figures 1–4. In all cases we find that the planes of both fragments are nearly perpendicular. There is no indication of an sp^2 character at the spiro centers as in the case of 1,3-diphenylspiro[imidazolidine-2,2'-indan]-1',3'-dione (**7**, R = Ph)[13] or ninhydrin[14].

In compounds **8**–**10** and **13** no significant differences of equivalent bond lengths and bond angles can be detected (Figures 1–4). The values obtained compare well with those of related species[15].

Compound **8** crystallizes with two disordered molecules in the asymmetric unit. The angles between both planes containing the spiro atom and the two neighboring atoms are 90.6 and 88.9°, respectively. The five-membered dioxolane rings have envelope conformations, and the indandione units are planar.

Compound **9** crystallizes with one disordered molecule in the asymmetric unit. The corresponding angle between both planes at the spiro atom is 85.1°. The oxathiolane ring deviates only weakly from an envelope conformation.

In the crystal, compound **10** is situated on a twofold crystallographic rotational axis. The five-membered dithiolane ring has a disordered twist conformation. The angle between the planes at the spiro carbon atom amounts to 90.2°.

Compound **13** crystallizes with two independent molecules A and B in the asymmetric unit. The molecular parameters of both molecules are identical within the limits of error. The angles between the planes at the spiro atoms are 90.2 and 88.6°, respectively. The half units connected by the spiro atom are almost planar. In the crystal of **13**, there is a close contact from the carbonyl O atom of A to the carbonyl C atom of B O3A···C12B 2.903(3) Å.

Photoelectron Spectra

The He(I) photoelectron (PE) spectra of **8**–**13** are interpreted by two approaches: Firstly, we try to correlate the

  0009–2940/94/1111–2215 $ 10.00+.25/0

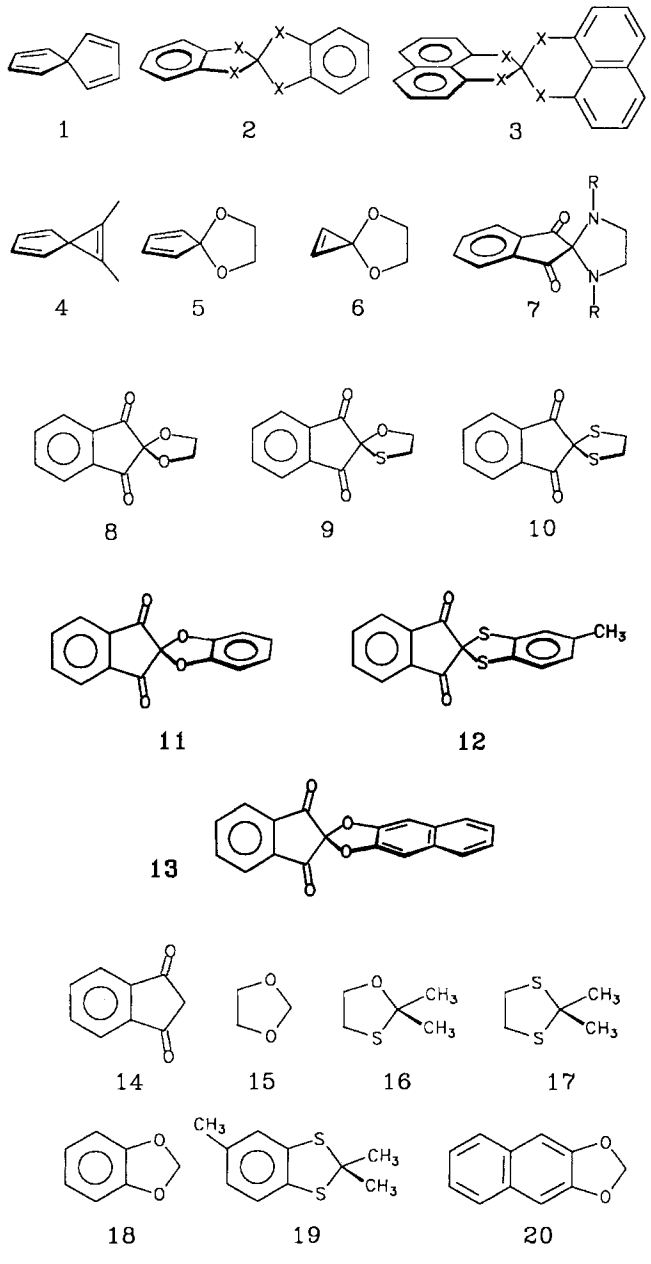

Scheme 1

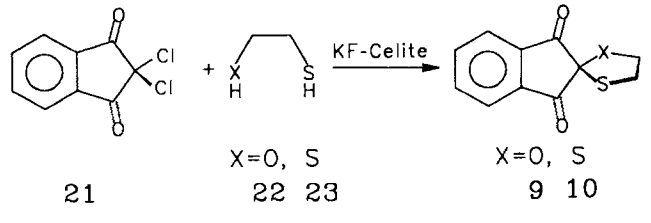

PE bands of **8**–**13** with those of the fragments **14**–**20**. Secondly, we correlate the PE bands with the orbital energies of molecular orbital (MO) calculations relying on Koopmans' approximation[16]. The methods used to derive the orbital sequence are either the MINDO/3[17] or the MNDO[18] procedures.

We start our discussion with the PE spectra of the fragments **14**–**20**. From these species the PE spectra of **14**[19],

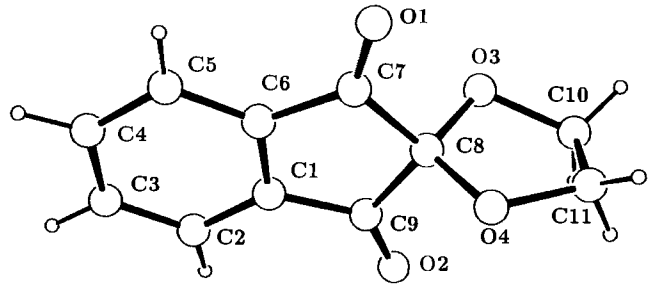

Figure 1. Molecular structure of **8** in the crystal. Only one of the two molecules in the asymmetric unit is shown without disorder. Selected bond lengths [Å] and angles [°]: C8–C7 1.539(3), C8–C9 1.536(3), C8–O3 1.411(3), C8–O4 1.392(3); C7–C8–C9 103.4(2), C9–C8–O4 110.1(2), C7–C8–O3 110.6(2), O3–C8–O4 107.7(2)

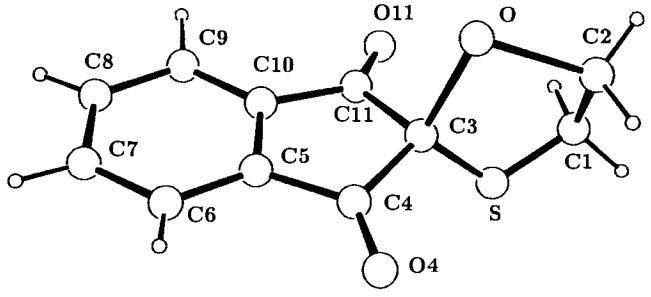

Figure 2. Molecular structure of **9** in the crystal. Only one of the disordered structures is shown. Selected bond lengths [Å] and angles [°]: C3–C4 1.543(2), C3–C11 1.541(2), C3–S 1.849(1), C3–O 1.393(2); C4–C3–C11 104.1(1), C11–C3–S 107.7(1), C4–C3–O 112.5(1), S–C3–O 108.3(1)

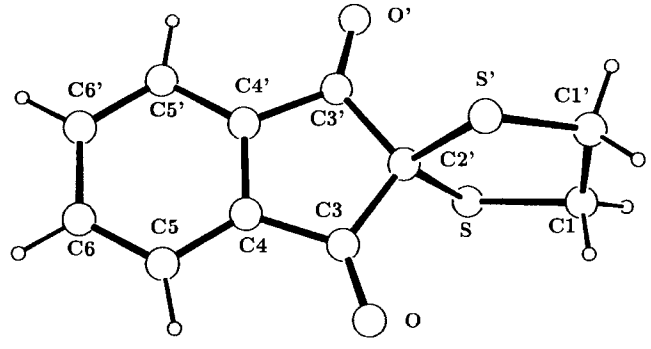

Figure 3. Molecular structure of **10** in the crystal. Only one of the disordered structures is shown. Selected bond lengths [Å] and angles [°]: C2′–C3 1.533(4), C2′–S 1.814(2); C3–C2′–C3′ 104.1(2), C3–C2′–S 110.72(8), S–C2′–S′ 109.2(2)

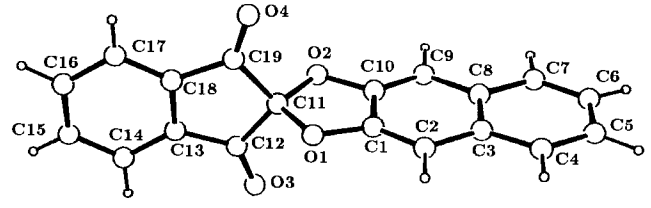

Figure 4. Molecular structure of **13** in the crystal. Only one of the disordered structures is shown. Selected bond lengths [Å] and angles [°]: C11–O1 1.419(3), C11–O2 1.424(2), C11–C19 1.533(3), C11–C12 1.538(3); C19–C11–C12 103.9(2), C19–C11–O1 112.6(1), C12–C11–O2 107.9(2), O1–C11–O2 107.9(2)

15[20], **17**[11b,21], **18**[6b], and **20**[6b] have been reported and their bands assigned. In the case of **14** the first three peaks at 9.36, 9.80, and 10.08 eV have been assigned to four bands arising from ionization from the lone-pair combinations $9b_2(n_-)$ and $12a_1(n_+)$ and two π ionizations, $2a_2(\pi)$ and $4b_1(\pi)$. In our correlations (see Figures 7 and 10) we use the PE values derived from **14a**, the 2,2-dimethyl congener of **14**. For **15** and **17** the first two bands arise from the 2p and 3p linear combinations. In the case of **15** the corresponding bands appear at 10.0 $[3b_1(\pi_+)]$ and 10.65 eV $[3b_1(\pi_-)]$. For **17** the corresponding bands are 8.77 $[3b_1(\pi_+)]$ and 9.12 eV $[2a_1(\pi_-)]$. The values reported for **18** are: 8.19 $[4b_1(\pi)]$, 9.14 $[2a_2(\pi)]$, and 10.99 eV $[3b_1(\pi)]$.The PE spectrum of **20**[6b] shows two peaks below 11 eV. Both are assigned to two transitions each, arising from π MOs. The PE spectra of 2,2-dimethyl-1,3-oxathiolane (**16**) and 2,2,5-trimethyl-1,3-benzodithiolane (**19**) are shown in Figure 5, the recorded ionization energies together with the assignments of both PE spectra are straightforward. In the case of the PE spectrum of **19** a comparison with the 2,2-dimethyl congener **19a**[6b] shows a very close agreement. The PE spectrum of **16** exhibits three bands below 11 eV. A comparison with the PE spectra of the closely related species **15** and **17** suggests to assign the first two bands to ionizations from the 3p- and 2p-type at sulfur and oxygen lone pairs, respectively. The third band corresponds to the ionization from an sp^2 sulfur lone pair.

The PE spectra of the spiro compounds **8**–**10** are shown in Figure 6. Common to all of them is a broad peak centered around 10 eV. From the ratios of the areas below the first few peaks we assign to the first peak in the PE spectrum of **8** one band, to the peak around 10 eV four bands, and to the shoulder at 10.5 eV one band again. In the PE spectrum of **9** the first two peaks are assigned to one band each and to the broad peak around 10 eV four bands. In the case of **10** the first peak at 8.7 eV is assigned to two strongly overlapping bands. The second peak around 10 eV is due to four bands. In Figure 7 the first bands of the PE spectra of **8**–**10** are compared with those of the fragments **14a**, **15**–**17**.

A comparison between the first PE bands of **14a**, **15**, and **8** suggests a considerable interaction between the fragments in **8**. Based on arguments from second-order perturbation theory one can rationalize the observed splitting pattern as follows: The replacement of the two methyl groups in **14a** by the dioxolane unit leads to a stabilization of the highest occupied MOs of the indandione moiety due to the higher electronegativity of oxygen as compared to carbon. This effect is opposed by the through-space interaction (spiro conjugation) of the two 2p orbitals (π_+-linear combination) of the dioxolane moiety with the lone pairs (n_--linear combination) of the carbonyl groups. This analysis is corroborated by the results of MO calculations shown in Figure 8. The comparison between the PE bands of **9** with those of **14a** and **16** indicates a slight stabilization of the PE bands of the indandione moiety. We ascribe this mainly to the inductive effect of the oxygen atom in **16**. In **10** the spiro interaction seems to dominate. It yields to a destabilization of the π_+ and π_- MOs localized at the sulfur atoms and to a stabilization of n_- and the other MOs of the indandione moiety. Our qualitative argumentation is confirmed by MO calculations as shown in Table 2.

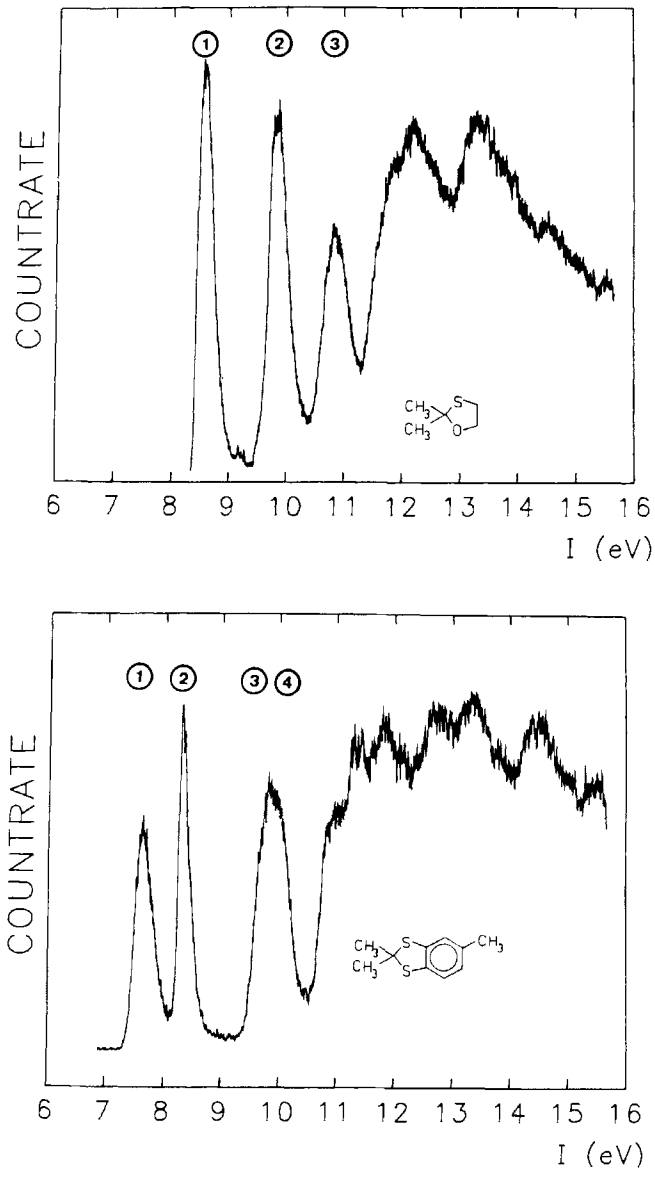

Figure 5. He(I) PE spectra of **16** and **19**

Table 1. Measured vertical ionization energies ($I_{v,j}$, eV) and calculated orbital energies ($-\varepsilon_j$, eV) of **16** and **19**

Compound	Band	$I_{v,j}$	Assignment	$-\varepsilon_j$ (MINDO/3)
16	1	8.60	$5a''(\pi_+,S)$	9.15
	2	9.90	$4a''(\pi_+,O)$	10.6
	3	10.90	$10a'(\sigma,S)$	9.86
19	1	7.65	$6b_1(\pi)$[a]	8.27
	2	8.30	$3a_2(\pi)$	8.89
	3	9.80	$2a_2(\pi)$	10.35
	4	10.1	$7b_2(\sigma)$	8.96

[a] The numbering refers to **19a** = **19** without 5-CH_3 (C_{2v}).

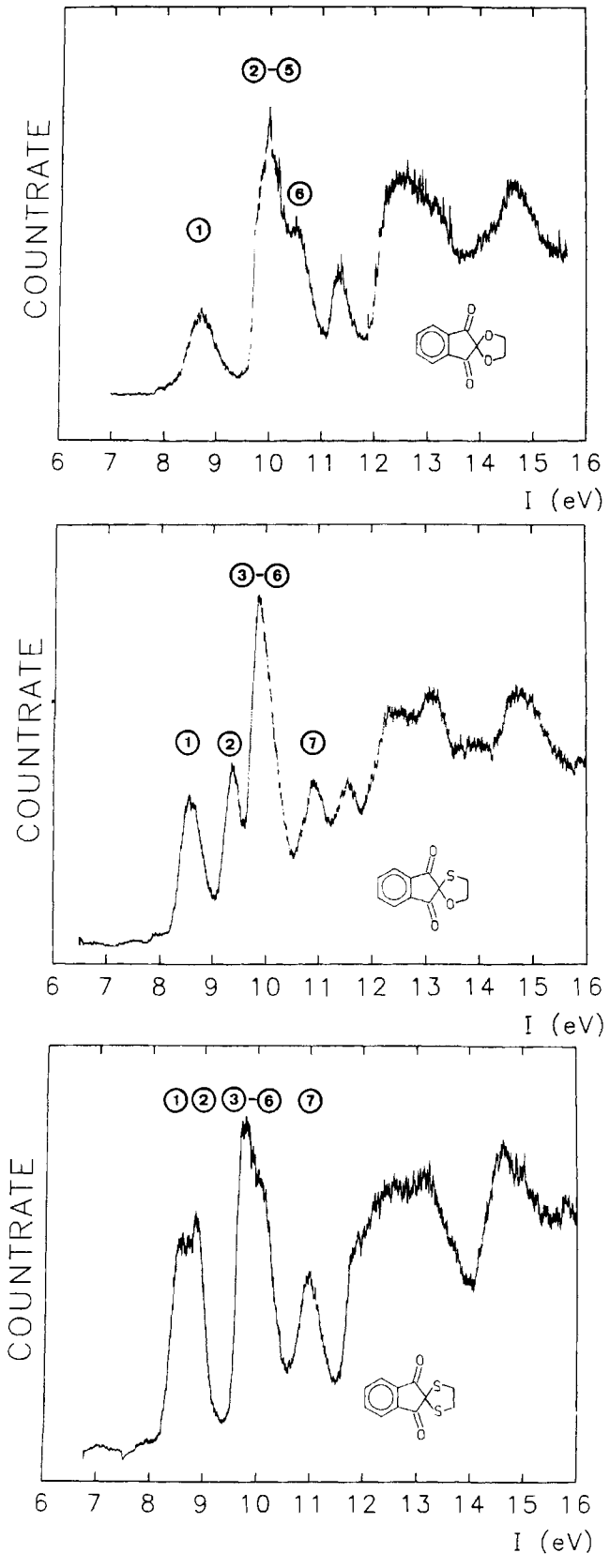

Figure 6. He(I) PE spectra of **8**–**10**

As anticipated from the discussion of the PE spectra of **8**–**10** we expect a broad peak around 10 eV in those of

Table 2. Measured vertical ionization energies ($I_{v,j}$, eV) and calculated orbital energies ($-\varepsilon_j$, eV) of **8**–**10**

Compound	Band	$I_{v,j}$	Assignment	$-\varepsilon_j$ (MINDO/3)
8	1	8.80	$11b_2(n-,\pi^+)$	8.67
	2	10.0	$4a_2(\pi)$	9.87
	3		$16a_1(n+)$	9.86
	4		$7b_1(\pi)$	9.98
	5		$3a_2(\pi)$	8.80
	6	10.50	$10b_2(\pi,n-)$	11.17
9	1	8.60	$15a''(\pi_+)$	8.80
	2	9.40	$14a''(n_-)$	9.38
	3	9.90	$13a''(\pi)$	9.63
	4		$13a''(\pi_-)$	9.86
	5		$22a''(n_+)$	9.97
	6		$12a''(n,p)$	10.94
	7	10.95	$21a'(\sigma)$	10.31
10	1	8.5	$11b_2(\pi_+)$	8.87
	2	8.70	$4a_2(\pi_-)$	9.30
	3	9.7 to 10.0	$7b_1(\pi)$	9.84
	4		$3a_3(\pi)$	9.75
	5		$16a_1(n_+)$	9.46
	6		$10b_2(n_-)$	10.08
	7	11.0	$6b_1(\sigma)$	9.21

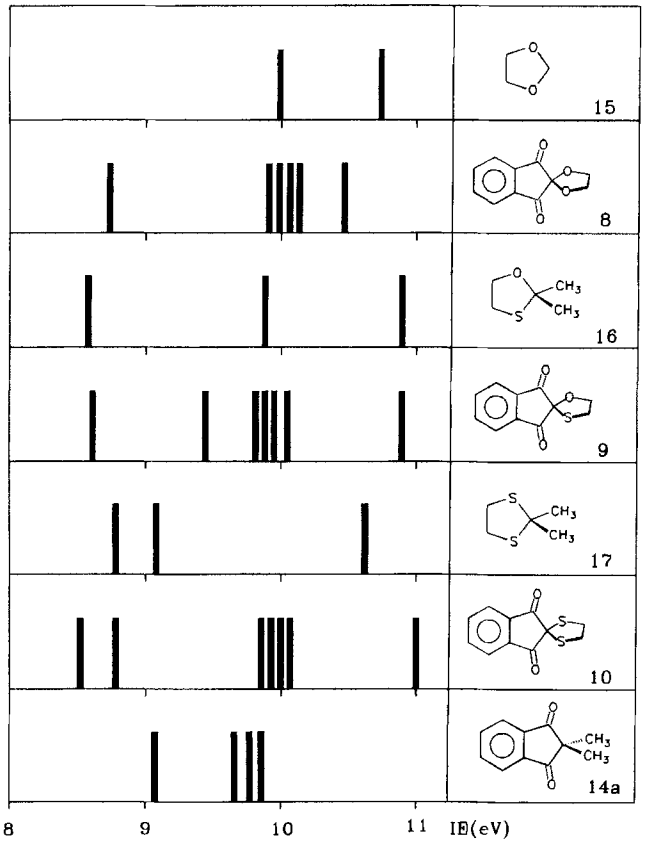

Figure 7. Comparison between the first PE bands of **8**, **9**, and **10** and those of the fragments **14a**–**17**. Each bar corresponds to one band

11–**13** due to the ionizations of the indandione fragment. This is indeed the case as shown in Figure 9. We assign the first three peaks in the PE spectrum of **11** to one transition each while we ascribe the two peaks centered at 10 eV to three bands. We notice a close similarity of bands 3–6 of

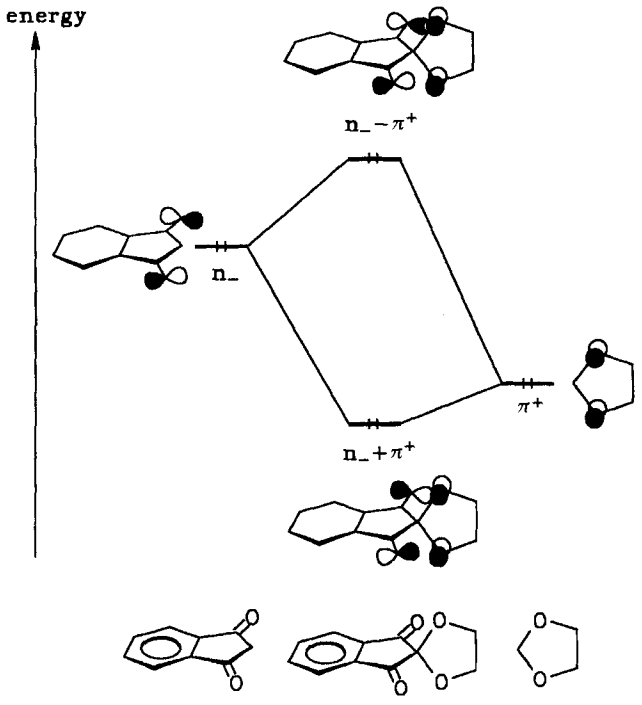

Figure 8. Schematic diagram demonstrating the interaction of the n_ MO of the indandione moiety with the π orbital of the 1,3-dioxolane fragment in **8**

11 to those of **14a** as concerns the shape of the bands and their ionization energies (see also Figure 10). In Figure 9 we also assign the first three peaks in the PE spectrum of **12** to a single band each, while the broad peak around 10 eV is assigned to five strongly overlapping bands. This judgement is based on the areas covered by the peaks. Similarly, we assign the first three peaks in the PE spectrum of **13** to two, one, and five bands, respectively.

A comparison of the PE bands of **11**–**13** with those of the fragments (see Figure 10) reveals a simple superposition of bands. In the case of **11** and **12** the first bands are slightly shifted, indicating a small interaction between the symmetrical π MO of the donor fragment and n_ as indicated in Figure 8.

The band sequence given in Figure 10 is confirmed by the MO calculations listed in Table 3. In the case of the MINDO/3 results a σ MO mainly centered at the sulfur atoms is predicted at rather low energy. However, a comparison with the PE spectra of other sulfur compounds[21] suggests to assign this lone pair to ionization events above 10 eV.

To conclude this paragraph we can say that with the exception of **8** and to a lesser extend **9** and **10** there is nearly no interaction between the two perpendicularly oriented moieties. The highest occupied molecular orbitals (HOMO) of **9**–**13** are strongly localized at the donor part.

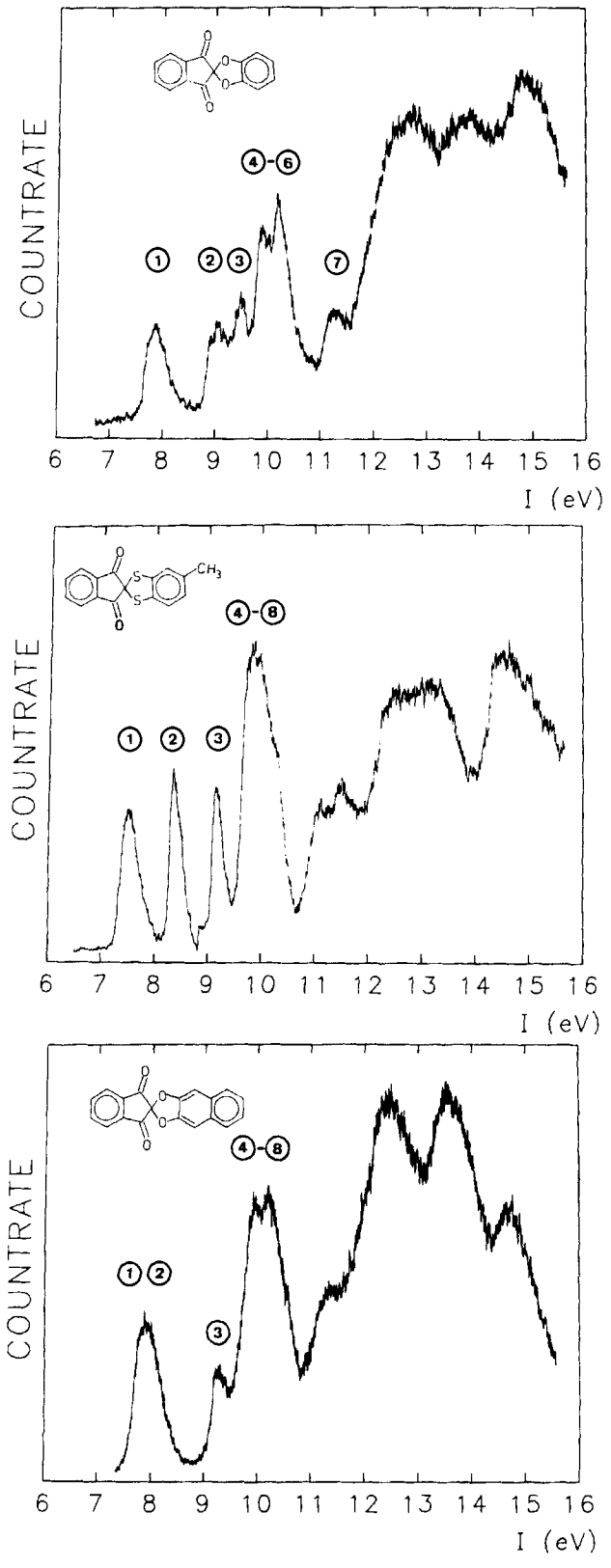

Figure 9. He(I) PE spectra of **11**–**13**

Electronic Absorption Spectra of 8–13

The electronic absorption spectra of **8**–**13** show a broad long wavelength absorption band around 25000 to 28000 cm^{-1} (band A) with low intensity, followed in part by a number of strongly overlapping bands with vibrational fine structure (bands B–G). The recorded data are listed in

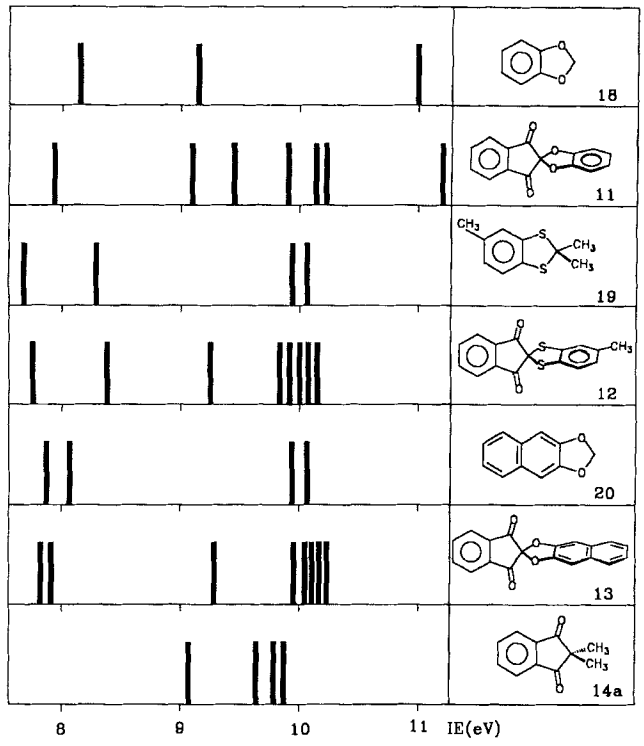

Figure 10. Comparison between the first PE bands of **11**–**13** and those of the fragments **14** and **18**–**20**. Each bar corresponds to one band

Table 3. Measured vertical ionization energies ($I_{v,j}$, eV) and calculated orbital energies ($-\varepsilon_j$, eV) of **11**–**13**

Compound	Band	$I_{v,j}$	Assignment	$-\varepsilon_j$ (MINDO/3)
11	1	7.9	$12b_2(\pi)$	8.05
	2	9.1	$4a_2(\pi)$	9.19
	3	9.5	$11b_2(n_-)$	9.17
	4	9.9	$3a_2(\pi)$	9.85
	5	10.2	$20a_1(n_+)$	9.78
	6		$10b_2(\pi)$	9.96
	7	11.3	$10b_1(\pi)$	11.32
12	1	7.58	$12b_2(\pi)$[a]	8.27
	2	8.48	$4a_2(\pi)$	8.95
	3	9.16	$11b_2(n_-)$	9.30
	4		$3a_2(\pi)$	9.73
	5	9.9	$9b_1(\pi)$	9.12
	6	to	$20a_1(n_+)$	9.39
	7	10.3	$10b_1(\sigma)$	9.12
	8		$2a_2(\pi)$	10.39
13	1	7.90	$5a_2(\pi)$	7.96
	2		$13b_1(\pi)$	8.07
	3	9.30	$12b_1(n_-)$	9.08
	4		$4a_2(\pi)$	9.87
	5	10.0	$24a_1(n_+)$	9.75
	6	to	$13b_2(\pi)$	9.98
	7	10.2	$3a_2(\pi)$	10.28
	8		$11b_1(\pi)$	10.91

[a] The numbering refers to the parent compound (C_{2v}).

Table 4. As examples we show in Figure 11 the UV/Vis spectra of **8**, **9**, **11**, and **13**.

A consideration of the UV/Vis data of **8**–**10** shows a three-band system (A, B, C) in which band B exhibits some vibrational fine structure. A comparison with that of **14a** shows (Figure 12) some similarity, as concerns the energy of the bands. The only difference is a larger energy gap between band A and B in **8**–**10** as compared to **14a**. A comparison between the UV/Vis spectra of **11**–**13** with those of **14a** or the aromatic fragments **18**–**20** (see Figure 12) shows a considerable long-wavelength shift of the low-energy band A.

To rationalize these observations we start our discussion with the assignment of the first UV bands of **14a**[1,23]. According to CNDO/S-CI calculations[24] the first two transitions in this molecule can be assigned to transitions from the two highest occupied MOs, the two linear combinations n_- and n_+ of the carbonyl oxygen lone pairs, to the lowest unoccupied MO (LUMO) which is the antisymmetric linear combination of the two π^* orbitals, mainly localized at the CO groups of the 1,3-dione moiety. In line with this assignment are the low intensity and the observation of a slightly hypsochromic shift of bands A and B of **14a** in changing the solvent from isooctane to methanol. Replacing the two CH_3 substituents in **14a** by the heterocycles as in **8**–**13** leads to a strong mixing between π_- and n_- as found for **8** (see Figure 8) or to a different HOMO, a π MO localized strongly at the donor fragment (**9**–**13**) as shown in the previous paragraph. Note that the energy of the HOMO in **8**–**10** is very similar to that of **14a** (c. f. Figure 7), but the wave function is strongly different. In **11**–**13** also the energy of the HOMO is higher than in **8**–**10** and **14a** and thus a pronounced long-wavelength shift of the first band is observed.

As a consequence of the difference in the wave function of the HOMO of **8**–**13** as compared to **14a** or the donor fragments **18**–**20** we expect a charge transfer character for band A in the electronic absorption spectra of **8**–**13**. To test this assignment, we have recorded the electron absorption spectra of **8**–**13** in solvents of different polarity such as benzene, acetonitrile, and methanol (Table 5). In Figure 13 we show as an example the result for **11**.

One finds a considerable hypsochromic shift for band A which is more pronounced for **11**–**13** as compared to **8**–**10**. This supports the assignment of the first band (band A) in the electronic absorption spectra of **8**–**13** as being due to a charge transfer process from the donor to the acceptor moiety.

This interpretation of the first band in the electronic absorption spectra of **8**–**13** is in line with earlier findings of Schönberg et al.[8c] and recently of Maslak et al.[10] who assigned the first band in 1,3-dialkyl- and 1,3-diarylspiro-[imidazolidine-2,2′-indan]-1′,3′-dione derivatives to a charge transfer process.

Conclusion

Our investigations reveal that only weak or no interactions occur between the two π moieties of the spiro compounds **8**–**13**. This finding is anticipated from other studies of spiro systems which show only a strong interaction when both fragments of the spiro system are identical such as in **1**–**3**[3–6]. The charge transfer character of the first band in the electronic absorption spectra also finds a simple ration-

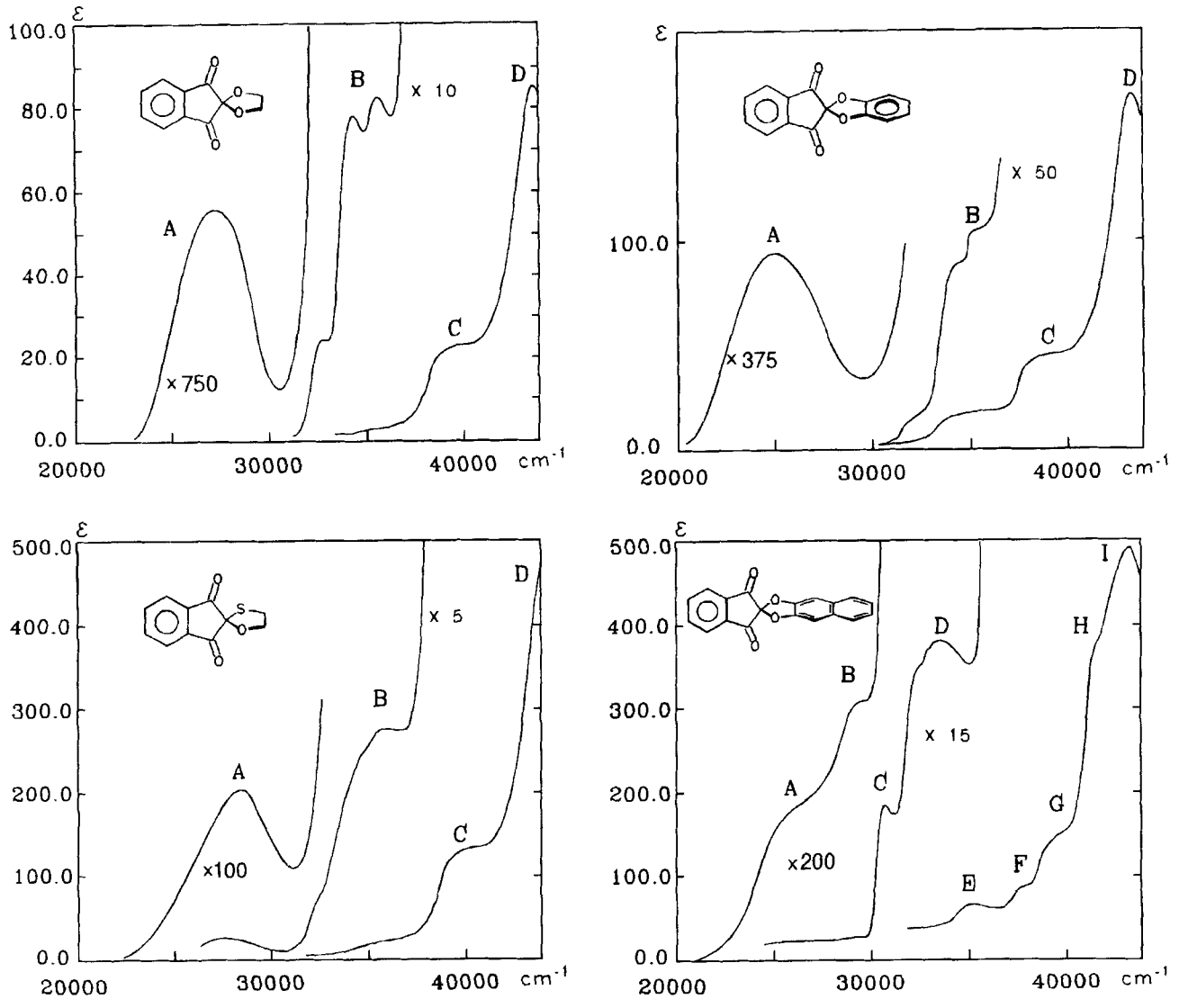

Figure 11. Electronic absorption spectra of **8**, **9**, **11**, and **13** in acetonitrile

alization: The LUMO is localized at the indandione moiety and the HOMO at the donor fragment.

We are grateful to the *Land Baden-Württemberg*, the *Fonds der Chemischen Industrie*, and the *BASF Aktiengesellschaft* for financial support. We thank *A. Flatow* for carrying out the PE measurements and Mrs. *P. Schlickenrieder* for typing the manuscript.

Experimental

Melting points (uncorrected): Dr. Tottoli (Büchi). – ^{1}H NMR ($CDCl_3$, tetramethylsilane as internal standard): 60 MHz: Varian EM 360; 90 MHz: Varian EM 390. – FD spectra: Finnigan MAT 311A. – IR: Beckman 4200. – He(I) PE spectra: Perkin Elmer, PS 18; calibration with Ar and Xe, 0.2 meV resolution on the $^2P_{3/2}$ line of Ar. – UV/Vis (acetonitrile unless noted otherwise): Cary 17D (Varian). – Elemental analyses: Mikroanalytisches Laboratorium der Chemischen Institute der Universität Heidelberg. – KF-Celite was prepared as described in ref.[22].

X-Ray Structure Analyses of the Spiro Compounds: Crystals of **8**, **9**, **10**, and **13** suitable for X-ray diffraction were selected. The X-ray data (Table 6) were collected at 298 K on an automated diffractometer (Enraf-Nonius CAD4, graphite monochromator, Mo-K_α radiation, ω-2Θ scan). Accurate cell parameters were determined by least squares techniques from selected Θ values. Lorentz and polarization effects were corrected. All structures were solved by direct methods (Multan[23]). The structural parameters were refined by full-matrix least-squares procedures on F with anisotropic thermal parameters for the carbon and hetero atoms. Hydrogen atoms were refined isotropically (Table 6). Compound **8** crystallizes with two disordered molecules in the asymmetric unit in the triclinic space group $P\bar{1}$, $Z = 4$. The ethylene group is disordered in a ratio of 1:1. C10 and C11 were refined isotropically. The hydrogen atoms were calculated according to stereochemical aspects. In refinement the parameters of these atoms were fixed. Compound **9** crystallizes with one disordered molecule in the asymmetric unit also in the triclinic space group $P\bar{1}$, $Z = 2$. The ethylene group is disordered in a ratio of 77:23. The parameters of the four hydrogen atoms in the disordered molecule (23%) during refinement were fixed. Compound **10** crystallizes with one disordered molecule in the asymmetric unit in the monoclinic space group $C2/c$, $Z = 4$. The molecule is situated on a twofold axis. The ethylene group is

Table 4. Long-wavelength bands of the electronic absorption spectra of **8**–**13** in acetonitrile

Compound	Band	$\tilde{\nu}$ [cm^{-1}]	λ [μm]	ε [l/mol·cm]
8	A	27100	369	52
	B	32790	305	258
		34480	290	777
		35460	282	830
	C	39840	251	11600
9	A	27930	358	207
	B	32790 (sh)	305 (sh)	506
		34620 (sh)	289 (sh)	1190
		35715	280	1315
	C	40485	247	12140
10	A	28760 (sh)	348 (sh)	227
	B	33000 (sh)	303 (sh)	900
		34365 (sh)	291 (sh)	1300
		35460	282	1350
	C	40000	250	11500
11	A	24885	402	92
	B	32380 (sh)	309 (sh)	380
		34840 (sh)	287 (sh)	4150
		37710	280	4920
	C	39000	256	15600
12	A	24650	406	353
	B	35125	285	6880
	C	39180	255	18570
13	A	25720 (sh)	389 (sh)	175
	B	29320 (sh)	341 (sh)	318
	C	30830	324	3230
	D	31650 (sh)	316 (sh)	4030
		32330 (sh)	309 (sh)	5300
		32860 (sh)	304 (sh)	5670
		33540	298	5750
	E	35345	283	7850
	F	36720 (sh)	272 (sh)	11750
	G	38450	260	24200
	H	40780	245	69600

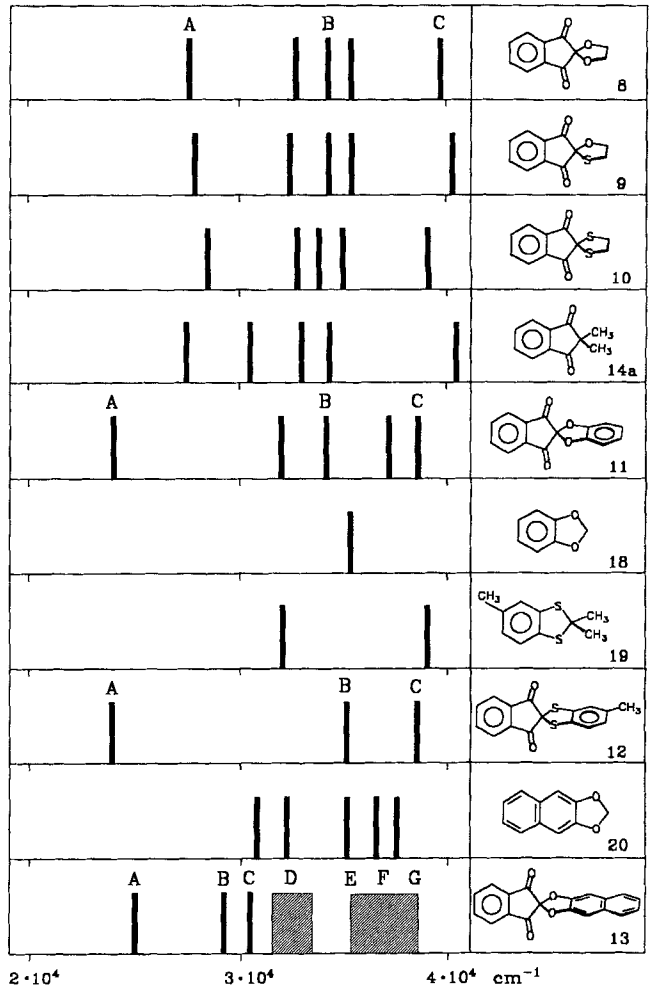

Figure 12. Comparison between the first bands in the electronic absorption spectra of **8**–**13** with those of the fragments **14a** and **18**–**20**. Each bar corresponds to one band

disordered in a ratio of 1:1. The eight hydrogen atoms of the disordered part of the molecule were calculated. In refinement the parameters of these atoms were fixed. Compound **13** crystallizes with two molecules in the asymmetric unit in the triclinic space group $P\bar{1}$, $Z = 4$.

Further details of the structure investigation are available on request from the Fachinformationszentrum Karlsruhe, Gesellschaft für wissenschaftlich-technische Information mbH, D-76344 Eggenstein-Leopoldshafen, on quoting the depository numbers CSD-400546, CSD-400545, CSD-400548, and CSD-400547, the names of the authors and the journal citation.

Spiro[indan-2,2'-[1,3]oxathiolan]-1,3-dione (**9**): To a solution of 4.3 g (20 mmol) of 2,2-dichloroindan-1,3-dione (**21**)[12] in 60 ml of dry acetonitrile were added 1.6 g (20 mmol) of 2-mercaptoethanol (**22**) and 11.6 g of KF-Celite (0.1 mol of KF)[22]. The mixture was stirred at 60°C for 3 h. After cooling the Celite was filtered off and washed (8 times) with acetonitrile. After solvent removal the residue was dissolved in 50 ml of THF, and the resulting solution was added to 150 ml of CH_2Cl_2. A dark-green precipitate was filtered off, and to the filtrate was added 100 g of silica gel 60 (0.063–0.200 mm). After the solvent had been removed by evaporation the residue was purified by column chromatography (silica gel, eluent THF) to yield 0.80 g (18%) of **9** as pale yellow crystals, m. p. 145–146°C (acetonitrile). – IR (KBr): $\tilde{\nu}$ = 1730 cm^{-1} (s), 1600 (m). – ^{1}H NMR (60 MHz) δ = 3.47 (t, J = 6 Hz, 2H, SCH_2), 4.75 (t, J = 6 Hz, 2H, OCH_2), 8.00 (s, 4H). – $C_{11}H_8O_3S$ (220.2): calcd. C 59.99, H 3.66, S 14.56; found C 60.09, H 3.69, S 14.58.

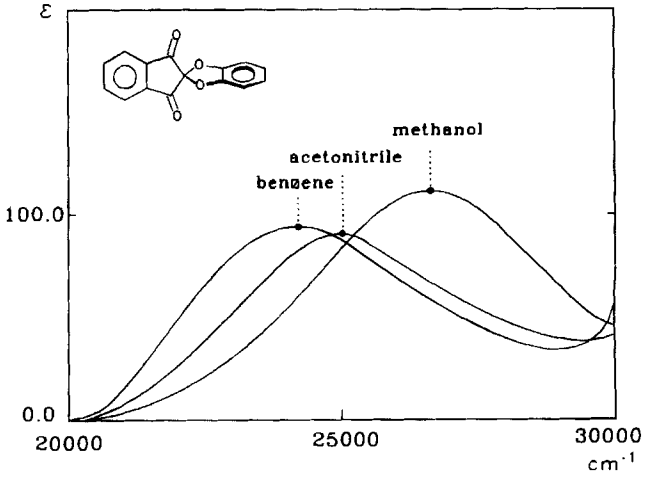

Figure 13. Long-wavelength band of the electronic absorption spectrum of **11** in benzene, acetonitrile, and methanol

Spiro[1,3-dithiolan-2,2'-indan]-1',3'-dione (**10**): Prepared from 4.3 g (20 mmol) of 2,2-dichloroindan-1,3-dione (**21**)[12] dissolved in

Table 5. Long-wavelength bands of the spiro compounds **8**–**13** in methanol, acetonitrile, and benzene in nm (ε)

Solvent	**8**	**9**	**10**
Methanol	365 (58)	356 (257)	–
Acetonitrile	369 (52)	358 (207)	348 (sh) (227)
Benzene	373 (58)	362 (353)	355 (sh) (227)
	11	**12**	**13**
Methanol	381 (110)	403 (394)	352 (sh) (200)
Acetonitrile	402 (92)	406 (353)	389 (sh) (175)
Benzene	415 (96)	412 (370)	400 (sh) (165)

Table 6. Crystallographic and refinement parameters of compounds **8**–**10** and **13**

Compound	**8**	**9**	**10**	**13**
formula	$C_{11}H_8O_4$	$C_{11}H_8O_3S$	$C_{11}H_8O_2S_2$	$C_{19}H_{10}O_4$
mol. mass [g]	204.2	220.3	236.3	332.4
crystal size [mm×10]	3×3.5×4.5	4.5×4×3.5	5×3×2.2	4.5×2×2
crystal system	triclinic	triclinic	monoclinic	triclinic
space group	$P\bar{1}$	$P\bar{1}$	$C2/c$	$P\bar{1}$
a [Å]	7.871(1)	7.492(1)	11.670(2)	10.506(2)
b [Å]	8.475(1)	8.273(1)	10.967(1)	10.716(2)
c [Å]	14.632(2)	9.097(1)	9.559(2)	13.497(2)
α [°]	81.86(1)	63.93(1)	90.00	94.86(2)
β [°]	88.39(1)	74.23(1)	122.37(1)	109.91(1)
γ [°]	77.65(1)	85.05(1)	90.00	86.98(1)
V [Å^3]	943.9(3)	487.1(1)	1033.3(6)	1423.0(9)
$D_{calc.}$ [Mg/m^3]	1.437	1.50	1.51	1.41
Z	4	2	4	4
$F(000)$	424	228	752	624
temperature [K]	298	298	298	298
$(\sin\theta/\lambda)_{max}$ [Å^{-1}]	0.66	0.66	0.66	0.59
μ [m^{-1}]	103.5	298.2	468.0	93.0
collected refl.	4882	3126	1318	5007
independent refl.	4557	2340	1245	4863
observed refl. [$I>2.5\sigma(I)$]	2610	2092	946	3374
no of variables	299	177	76	495
$(\Delta/\sigma)_{max}$	0.02	< 0.01	0.01	< 0.01
R	0.053	0.04	0.053	0.041
R_w	0.064	0.061	0.081	0.049
$(\Delta\rho)_{max}$ [eÅ^{-3}]	0.23	0.46	0.48	0.17
$(\Delta\rho)_{min}$ [eÅ^{-3}]	-0.35	-0.38	-0.47	-0.22

60 ml of acetonitrile and 2.0 g (20 mmol) of 1,2-dimercaptoethane (**23**) and 11.6 g of KF-Celite[22] (0.1 mol of KF) by using the same procedure as for the synthesis of **9**. After the solvent had been removed the residue was dissolved in 50 ml of THF and the resulting solution poured into 200 ml of CH_2Cl_2. The brown precipitate was removed by filtration. After the solvent had been removed, the residue was dissolved in benzene, the solution filtered again, and the filtrate concentrated until crystallization started. This procedure afforded 1.2 g (25%) of **10** as pale yellow crystals, m. p. 177–178°C. – IR (KBr): $\tilde{\nu}$ = 1710 cm^{-1} (s), 1645 (m), 1590 (m). – ^{1}H NMR (90 MHz): δ = 3.75 (s, 4H, CH_2CH_2), 8.00 (m, 4H). – $C_{11}H_8O_2S_2$ (236.3): calcd. C 55.91, H 3.41, S 27.14; found C 55.82, H 3.43, S 27.26.

Spiro[1,3-benzodioxol-2,2'-indan]-1',3'-dione (**11**): Prepared from 1.1 g (10 mmol) of *o*-dihydroxybenzene dissolved in 30 ml of dry acetonitrile, 2.15 g (10 mmol) of 2,2-dichloroindan-1,3-dione (**21**)[12] and 5.8 g of KF-Celite (50 mmol of KF)[22]. The mixture was stirred at 60°C for 4 h. After the solvent had been removed the residue was chromatographed on silica gel 60 (0.063–0.200 mm, eluent CH_2Cl_2). The yellow fraction yielded 1.8 g (71%) of **11** as yellow crystals, m.p. 164–165.5°C (acetonitrile). – IR ($CHCl_3$): $\tilde{\nu}$ = 1800 cm^{-1} (w), 1775 (s), 1745 (s), 1610 (m). – ^{1}H NMR (90 MHz): δ = 6.95 (s, 4H), 8.05 (m, 4H). – $C_{15}H_8O_4$ (252.2): calcd. C 71.43, H 3.20; found C 71.48, H 3.40.

5-Methylspiro[1,3-benzodithiol-2,2'-indan]-1',3'-dione (**12**): Prepared from 1.6 g (10 mmol) of toluene-2,4-dithiol, 2.15 g (10 mmol) of 2,2-dichloroindan-1,3-dione (**21**)[12], and 5.8 g of KF-Celite (50 mmol of KF)[22] in 30 ml of acetonitrile according to the same procedure as for **9**–**11**. The yellow-orange fraction yielded 1.1 g (37%) of **12**, m.p. 183–183.5°C. – IR (KBr): $\tilde{\nu}$ = 1750 cm^{-1} (w), 1715 (s), 1595 (m), 1465 (m). – ^{1}H NMR (60 MHz): δ = 2.30 (s, 3H, CH_3), 7.0 (m, 3H), 8.05 (m, 4H). – $C_{16}H_{10}O_2S_2$ (298.4): calcd. C 64.40, H 3.38, S 21.49; found C 64.19, H 3.49, S 21.59.

Spiro[indan-2,2'-naphtho[2,3-d]-1,3-dioxol]-1,3-dione (**13**): Prepared by treatment of 1.0 g (6.25 mmol) of 2,3-dihydroxynaphthalene with 1.1 g (5 mmol) of **21**[12] and 2.9 g of KF-Celite (25 mmol of KF)[22] in 30 ml of acetonitrile at 60°C for 8 h by using the same procedure as for **9**. The Celite was washed with hot CH_2Cl_2. After the organic solvent had been removed the residue was chromatographed on silica gel. The yellow fraction yielded 0.60 g (40%) of **13** as yellow needles, m.p. 235–236°C (acetonitrile). – IR (KBr): $\tilde{\nu}$ = 1788 cm^{-1} (w), 1762 (s), 1728 (s), 1594 (m), 1472 (s). – ^{1}H NMR (90 MHz): δ = 7.15–7.45 (m, 4H), 7.70 (m, 2H), 8.10 (m, 4H). – $C_{19}H_{10}O_4$ (302.3): calcd. C 75.49, H 3.34; found C 75.25, H 3.45.

☆ Dedicated to Professor *Wolfgang Lüttke* on the occasion of his 75th birthday.

[1] H. E. Simmons, T. Fukunaga, *J. Am. Chem. Soc.* **1967**, *89*, 5208.
[2] R. Hoffmann, A. Imamura, G. D. Zeiss, *J. Am. Chem. Soc.* **1967**, *89*, 5215.
[3] Review: H. Dürr, R. Gleiter, *Angew. Chem.* **1978**, *90*, 591; *Angew. Chem. Int. Ed. Engl.* **1978**, *17*, 559.
[4] C. Batich, E. Heilbronner, E. Rommel, M. F. Semmelhack, J. S. Foos, *J. Am. Chem. Soc.* **1974**, *96*, 7662.
[5] A. Schweig, U. Weidner, R. K. Hill, D. A. Cullison, *J. Am. Chem. Soc.* **1973**, *95*, 5426.
[6] [6a] R. Gleiter, R. Haider, H. Quast, *J. Chem. Res. (S)* **1978**, 138. – [6b] R. Gleiter, J. Uschmann, *J. Org. Chem.* **1986**, *51*, 370. – [6c] J. Spanget-Larsen, J. Uschmann, R. Gleiter, *J. Phys. Chem.* **1990**, *94*, 2334.
[7] P. Bischof, R. Gleiter, H. Dürr, B. Ruge, P. Herbst, *Chem. Ber.* **1976**, *109*, 1412.
[8] [8a] A. Schönberg, E. Singer, M. Osch, G.-A. Hoyer, *Tetrahedron Lett.* **1975**, 3217. – [8b] A. Schönberg, E. Singer, B. Eschenhof, G.-A. Hoyer, *Chem. Ber.* **1978**, *111*, 3058. – [8c] A. Schönberg, E. Singer, *Tetrahedron* **1978**, *34*, 1285.
[9] G. Hohlneicher, *Ber. Bunsenges. Phys. Chem.* **1967**, *71*, 917; W. Trischler, E. Sturm, H. Kiesele, E. Daltrozzo, *Chem. Ber.* **1984**, *117*, 2703.
[10] P. Maslak, A. Chopra, *J. Am. Chem. Soc.* **1993**, *115*, 9331.
[11] [11a] J. Spanget-Larsen, R. Gleiter, R. Haider, *Helv. Chim. Acta* **1983**, *66*, 1441. – [11b] M. Kobayashi, R. Gleiter, D. L. Coffen, H. Bock, W. Schulz, H. Stein, *Tetrahedron* **1977**, *33*, 433.
[12] A. Schwarz, G. Uray, H. Junek, *Liebigs Ann. Chem.* **1980**, 1919.
[13] W. S. Sheldrick, A. Schönberg, E. Singer, *Acta Crystallogr., Sect. B*, **1982**, *38*, 1355.
[14] R. C. Medrud, *Acta Crystallogr., Sect. B*, **1969**, *25*, 213.
[15] H. P. Weber, E. Galantay, *Helv. Chim. Acta* **1972**, *55*, 544; G. Bravic, J. Gaultier, C. Hauw, *Cryst. Struct. Commun.* **1974**, *3*, 219; D. K. Banerjee, J. Alexander, A. V. Abraham, K. Venkatesan, T. N. G. Row, *Indian J. Chem.* **1976**, *14*, 145; J. H. Noordik, L. Groen, *Cryst. Struct. Commun.* **1978**, *7*, 293; G. P. Chiusoli, G. Salerno, E. Bergamaschi, G. D. Andreetti, G. Bocelli, P. Sgarabotto, *J. Organomet. Chem.* **1979**, *177*, 245; P. S. White, D. C. N. Swindells, *Acta Crystallogr., Sect. B*, **1980**, *36*, 491.
[16] T. Koopmans, *Physica* **1934**, *1*, 104.
[17] R. C. Bingham, M. J. S. Dewar, D. H. Lo, *J. Am. Chem. Soc.* **1975**, *97*, 1285; P. Bischof, *ibid.* **1976**, *98*, 6844.

[18] M. J. S. Dewar, W. Thiel, *J. Am. Chem. Soc.* **1977**, *99*, 4899.
[19] V. Galasso, F. P. Colonna, G. Distefano, *J. Electron Spectros. Relat. Phen.* **1977**, *10*, 227.
[20] D. A. Sweigart, D. W. Turner, *J. Am. Chem. Soc.* **1972**, *94*, 5599.
[21] R. Gleiter, J. Spanget-Larsen, *Top. Curr. Chem.* **1979**, *86*, 139.
[22] J. Yamawaki, T. Ando, *Chem. Lett.* **1979**, *45*, 755.
[23] K. H. Giovanelli, J. Dehler, G. Hohlneicher, *Ber. Bunsenges. Phys. Chem.* **1971**, *75*, 864.
[24] J. Del Bene, H. H. Jaffé, *J. Chem. Phys.* **1968**, *48*, 1807.

[152/94]